

REPORT DOCUMENTATION PAGE					Form Approved OMB No. 0704-0188	
<p>The public reporting burden for this collection of information is estimated to average 1 hour per response, including the time for reviewing instructions, searching existing data sources, gathering and maintaining the data needed, and completing and reviewing the collection of information. Send comments regarding this burden estimate or any other aspect of this collection of information, including suggestions for reducing the burden, to Department of Defense, Washington Headquarters Services, Directorate for Information Operations and Reports (0704-0188), 1215 Jefferson Davis Highway, Suite 1204, Arlington, VA 22202-4302. Respondents should be aware that notwithstanding any other provision of law, no person shall be subject to any penalty for failing to comply with a collection of information if it does not display a currently valid OMB control number.</p> <p>PLEASE DO NOT RETURN YOUR FORM TO THE ABOVE ADDRESS.</p>						
1. REPORT DATE (DD-MM-YYYY) 14-06-2003		2. REPORT TYPE Final Technical Report		3. DATES COVERED (From - To) From 01-06-98 To 30-09-2002		
4. TITLE AND SUBTITLE Novel Experimental, Theoretical, and Calculational Approaches to Understanding the Detonation of Explosives				5a. CONTRACT NUMBER N/A		
				5b. GRANT NUMBER N0014-98-1-0736		
				5c. PROGRAM ELEMENT NUMBER		
				5d. PROJECT NUMBER 02PR12665.00		
				5e. TASK NUMBER		
				5f. WORK UNIT NUMBER		
7. PERFORMING ORGANIZATION NAME(S) AND ADDRESS(ES) University of Nebraska-Lincoln Lincoln, NE 68588				8. PERFORMING ORGANIZATION REPORT NUMBER		
9. SPONSORING/MONITORING AGENCY NAME(S) AND ADDRESS(ES) Office of Naval Research Regional Office - San Diego 4520 Executive Drive, Suite 300 San Diego, CA 92121-3019				10. SPONSOR/MONITOR'S ACRONYM(S)		
				11. SPONSOR/MONITOR'S REPORT NUMBER(S)		
12. DISTRIBUTION/AVAILABILITY STATEMENT APPROVED FOR PUBLIC RELEASE						
13. SUPPLEMENTARY NOTES						
14. ABSTRACT Report of results of research on the initial stage of detonation is made. Experimental results involve location of a heretofore undetected intramolecular mode in RDX and confirmation of prior findings on the Raman scattering of HMX. Preliminary Brillouin scattering studies have permitted experimental determination of approximate values of all components of the HMX crystals' stiffness tensor. The results of a mechanochemical theory are presented. The model account for the initial stage of detonation involving molecular decomposition. Symmetry arguments based on the theory show that high symmetry molecules will be inherently less stable under compression than higher symmetry ones. The mechanochemical model also offers a direct explanation of the role of hot spots in detonation.						
15. SUBJECT TERMS Detonation, RDX, HMX, Raman scattering, Brillouin scattering, Stiffness tensor, mechanochemistry, hot spots						
16. SECURITY CLASSIFICATION OF: a. REPORT UU			17. LIMITATION OF ABSTRACT SAR	18. NUMBER OF PAGES 9	19a. NAME OF RESPONSIBLE PERSON Craig J. Eckhardt 19b. TELEPHONE NUMBER (Include area code) (402)-472-2734	

Introduction to Research Aims

The goal of this ONR-sponsored research was to obtain the phonon spectra and elastic constants for crystals of the explosives HMX, RDX and CL20 by vibrational spectroscopy. The spectroscopies used were Raman and Brillouin scattering. Another objective was to measure the modal strain Grüneisen parameters of these systems using piezomodulated Raman scattering. All of these data are crucial to the development and testing of current models of detonation that are concerned with the initial transfer of mechanical energy into molecular degrees of freedom. The intent was to accompany these measurements with a more developed, quantitative microscopic theory that would address how the mechanical energy of a shock wave, for example, is converted into chemical energy at the very initial phase of the detonation process. Once this energy causes initial chemical processes, the mechanism of detonation then becomes simultaneously more complex but also more in tune with current theory, methodologies and findings. However, it is the microscopic nature of the process at this initial stage that is crucial since its understanding may be expected to assist chemists to synthesize new molecules of energetic materials that possess decreased sensitivity to detonation with increased detonation power.

Since it is well-known that different crystalline forms of an energetic material possess different sensitivities to detonation, the collective behavior of the molecules in a crystal must also be understood for effective design of new energetic materials. Thus, the measurements and the model must tie the molecular properties to those of the aggregate, the matrix or crystal. Although most energetic materials are most commonly embedded in amorphous solids, the crystalline forms were focused upon because they afford a simpler and more quantifiable system from which a model may be built. Once formulated, such a model should be capable of extension to amorphous composites.

While practical explosives are usually comprised of energetic materials suspended in a matrix, usually a polymeric material, the fundamental microscopic process at the initial phase of detonation may be expected to be essentially independent of the specific environment of the molecule. Under this assumption, the model developed in this research to explain the microscopic process treats the surroundings of a given molecule in a solid phase as being embedded in a continuous medium that may be represented by a mechanical susceptibility. Since this mechanical susceptibility may be anisotropic, it is represented by a tensor that is itself related to the elastic properties of the material.

The experimental techniques used in the research required large, well-formed single crystals of very high optical quality for successful measurements. This proved to be a major barrier to the progress of the research and to completion of its goals. Over half of the grant period was exhausted in obtaining requisite samples and clearing the legal obstacles for their acquisition, shipping, storage and study. Once obtained in sufficient quantity, the next difficulty was in developing a successful methodology for generating crystals of the needed polymorph, size (minimally 2mm on an edge), optical quality and morphology.

Studies of RDX

The literature states the preferred method for growth of single crystals of RDX is by slow evaporation from a saturated solution of acetone. Using this method, we were able to grow single crystals, but they were small and had far too many tiny faces to be useful in Raman and Brillouin spectroscopy. We instead chose to grow RDX single crystals from a solution of cyclohexanone saturated with deionized water. A combination of gradual temperature lowering and evaporation resulted in large crystals with eight faces zonal to the crystallographic *b* axis. These crystals were clear, colorless, and visually defect free. Optical goniometry revealed that two major forms, {00-1}

and {100}, that allowed easy study of the different elements of the Raman polarizability tensor.

The previous polarized Raman study on RDX was performed by Rey-Lafon *et al.* in 1971.¹ They probed the region from 3200 cm⁻¹ to 10 cm⁻¹. There are 57 possible internal vibration modes in a RDX molecule and 24 Raman-active lattice modes. Rey-Lafon *et al.* were able to identify 45 molecular modes and to locate most of the lattice modes. Our work studied the region from 3300 cm to 10 cm⁻¹. We have located all 57 molecular modes and all 24 of the lattice modes. Our most notable finding here is the identification of a sharp fundamental at 3233 cm⁻¹ that was previously unreported by other researchers. Our instrumentation allows us to scan with a resolution greater than 1 cm⁻¹, which aided in the location of modes that were apparently missed in the previous study.

Growth & Characterization of HMX and TNAZ

Single crystals of HMX were grown using two methods. The first involved gradually lowering the temperature of a saturated solution of HMX in acetone. The temperature of the solution was controlled by thermal contact with a water jacket. The entire apparatus was thermally isolated to diminish any undesirable fluctuations in temperature. The temperature was incrementally decreased at intervals of 1 C° per day until the appearance of small seed crystals. At this point, the cooling rate was decreased to 0.1 C° per day until sufficiently large crystals were grown. If the cooling was too rapid, the crystals would grow poorly and the process would need to be repeated. The second method involved an evaporative technique. Rather than gradual cooling, the saturated solution was maintained at a constant temperature while the solvent, acetone, was slowly evaporated. This method produced a well-formed crystal within approximately two weeks. Compared to the gradual cooling method, these crystals were grown relatively quickly, therefore, the evaporative method was predominantly used. Visual examination showed crystals of good optical quality.

After the crystals were grown, their structures were determined by X-ray diffraction measurements that confirmed a non-solvated, β -HMX polymorph, with space group and lattice constants consistent with those previously reported.¹ None of the other polymorphs were observed. The β -polymorph crystals grew with a habit of faces zonal to the “ a ” crystallographic axis. The zonal and capping faces were determined with optical goniometry and later verified by X-ray diffraction.

The crystallization of TNAZ has been more difficult. Since evaporation worked well for HMX, a similar approach was adopted for TNAZ. Initially, CCl₄ was used as a solvent. As the solvent evaporated, no seed crystals would form and eventually, the solute would solidify in either a powder or a poorly formed crystalline plate, neither of which, is of any use to this study. Therefore, other solvents were studied, including, methylene chloride and chloroform. Although the use of these solvents afforded similar results to carbon tetrachloride, it was observed that the point at which the solute would solidify was very different. Methylene chloride solutions could continue to evaporate until a highly saturated solution of TNAZ would effectively precipitate. However, when chloroform was used, large plate-like crystals, albeit poor, would form much earlier. Therefore, varying mixtures of chloroform and methylene chloride were used. To date, the most successful solution was approximately 80% chloroform and 20% methylene chloride. Unfortunately, the harvested crystals still had too many defects for any use in spectroscopy.

Studies of β -HMX

Crystal Optics

β -HMX, which is a monoclinic polymorph,² requires a complete optical indicatrix in order to account for any optical anisotropy. To accomplish this, near-normal incident specular reflectivity was measured at 514.5 nm for three symmetrically inequivalent faces. This wavelength was used for two

reasons. First, since the β -HMX crystals are transparent, the imaginary part of the complex refractive index can be neglected. Thus, Fresnel's Law for reflectivity is only a function of the refractive index. Second, this wavelength is the excitation wavelength used in both Raman and Brillouin experiments. Thus, considering any dispersion of the refractive index with wavelength is unnecessary. By measuring the reflectivity of light polarized along the principal directions of each symmetrically inequivalent face, corresponding refractive indices could be calculated using Fresnel's Law. In turn, this data allows determination of the semi-axes of the optical indicatrix, which are: $n_\alpha = 1.58$, $n_\beta = 1.67$ and $n_\gamma = 1.80$ and from which the refractive index along any direction rystal can be calculated.

Raman Spectroscopy of β -HMX

Single-crystal, polarized, Raman spectra of β -HMX were recorded from 30 to 3000 cm^{-1} with varying polarizations used to assign modal symmetries. The intramolecular modes agree [see Fig. 1] with those previously reported.³ The lattice modes assignments (spectra shown in Fig. 2) agreed with those reported by Iqbal, *et al.*³ and not those reported by Cavagnat, *et al.*⁴ and Brill, *et al.*⁵

Beside these experimental studies, we have also calculated the Raman lattice frequencies. The calculation involved an empirically fit, 6-exp Buckingham potential which is a function of twelve variables: six lattice constants, three translations and three Euler angles that describe the relative orientation of molecular inertial axes to the orthogonal crystallographic axes. The lattice energy was initially calculated from these variables as well as the atomic coordinates and then minimized with respect to the initial crystallographic parameters. The quality of the chosen potential parameters was judged on how well the lattice parameters minimize the energy compared to experimental parameters. If any of the lattice parameters changed by more than approximately 0.5 \AA , the potential was modified to more accurately reproduce experimental data.

Once the atomic coordinates are in the correct frame of reference, a suitable lattice needs to be constructed. Generally, a lattice consisting of 150 molecules will provide an adequate representation of the crystal. The lattice used for this study was a 4x4x4 unit cell cube. The initial potential parameters chosen for this system were those of three groups: Sorescu, *et al.*,⁶ Smith, *et al.*⁷ and Gavezzotti.⁸ Although the first two groups' potentials focused primarily on nitramine-type molecular crystals, the more general parameters reported by Gavezzotti gave a minimized lattice energy of 33 kcal/mol which was the closest to the experimentally determined heat of sublimation of 41 kcal/mol.⁹ Although the Raman frequencies calculated using Gavezzotti's parameters did not compare particularly well with experiment, his potential provides a starting point.

The potential parameters were modified through an iterative trial and error process. This process was continued until the lattice constants, corresponding to a minimized energy, were comparable to experimental ones. The minimized lattice energy was calculated to be 33.7 kcal/mol and the calculated frequencies, shown compared well with those found experimentally by Iqbal *et al.* and us.

The results obtained over the period of the grant indicate that the direction of the research was pursuing would lead to further refinement and correction of data already in the literature. Further, the main purpose in obtaining the Raman scattering data was for its necessary combination with the results of the intended piezomodulated Raman scattering data to yield the anisotropic strain Grüneisen parameters that are critical to the development of any understanding of the role of shock or stress in the initial phase of mechanical detonation of energetic materials. Unfortunately, the period of the grant expired before the piezomodulated Raman scattering work could be initiated.

HMX B_g Symmetry Optical Modes

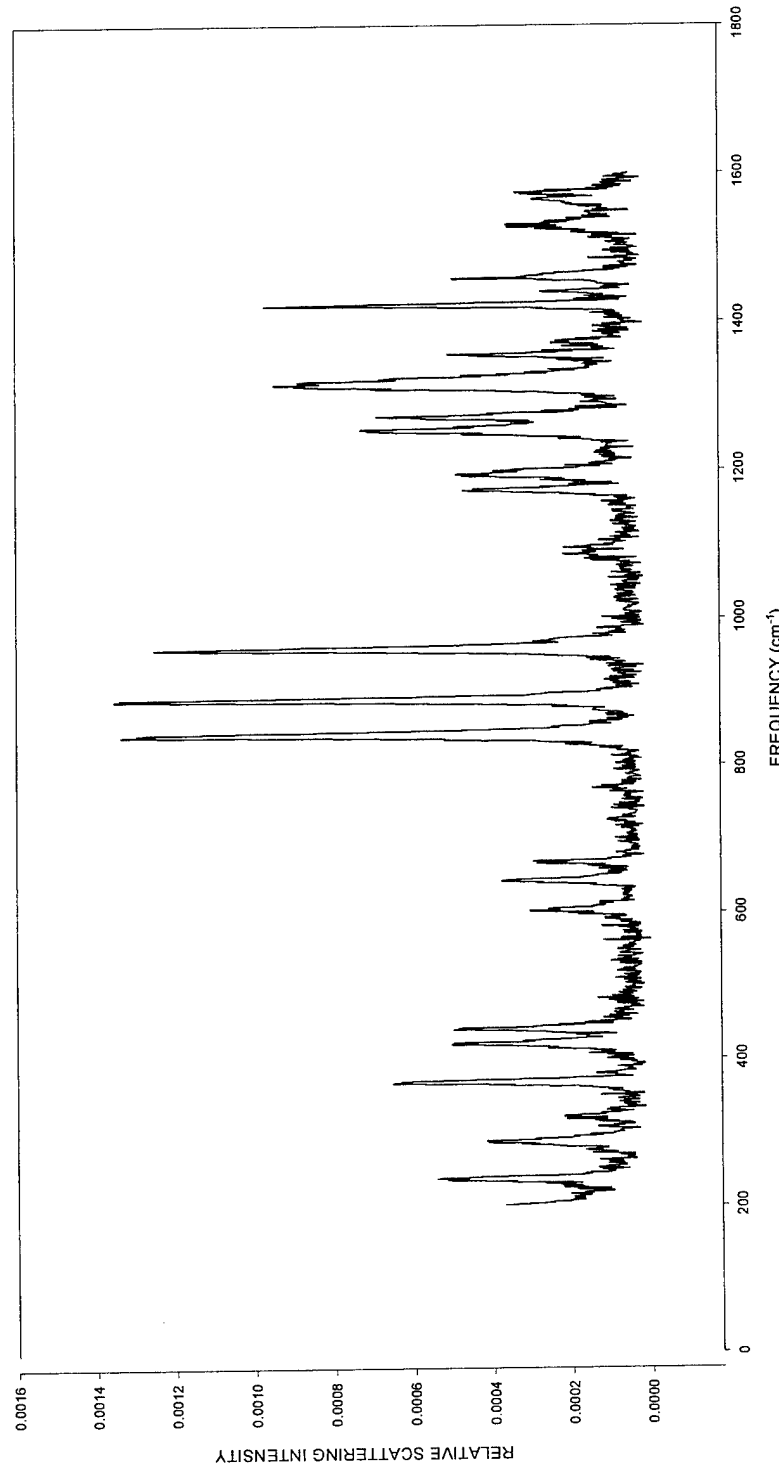


Figure 1: Raman scattering of B_g symmetry optical (molecular) modes of β -HMX.

Raman Scattering of Lattice Modes of HMX

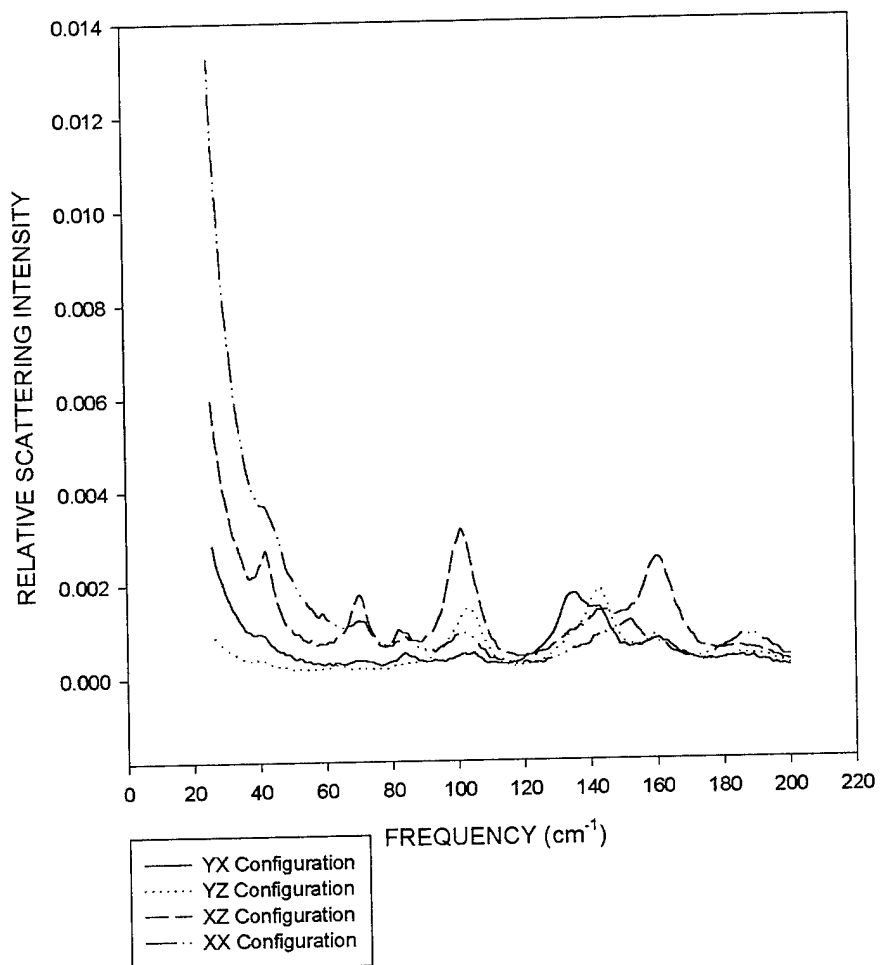


Figure 2: Raman scattering of lattice modes of β -HMX for four different scattering configurations.

Brillouin Spectroscopy

Brillouin scattering measurements were made for directions associated with all naturally occurring pairs of symmetrically inequivalent zonal faces. The low symmetry of most organic crystals affords only a minimal number of elastic constants to be directly calculated from acoustic velocities. For a monoclinic system, the longitudinal velocity for the [010] phonon is directly related to the C_{22} elastic constant. However, difficulty remains in the calculation of the remaining 12 elastic constants. A solution involves an over-determined set of phonons for solving the equations of the Christoffel determinant. The experimental data for each scattering geometry include the direction cosines of the phonon wavevector, the refractive index of the incident and scattering wavevector and the measured Brillouin shifts, which are used to calculate the phonon's velocity in the $\mathbf{k} = 0$ approximation. This data is then input into a minimization program. An initial stiffness matrix is then incrementally minimized until the calculated values best reproduce the experimental ones.

However, for the scattering experiments we performed, the determinant of the calculated elastic constant matrix was not positive-definite which indicates a nonphysical system. Since the scattering geometries used involved pairs of faces zonal to the a crystallographic axis, scattering was constrained to the bc^* plane. Based on the poor convergence of the stiffness matrix, the elastic anisotropy of HMX cannot be fully described using phonons of a single plane. Therefore, adaptations to the Brillouin spectrometer were made that facilitated the measurement of non-zonal capping faces. Besides simply increasing the number of scattering geometries, using phonons of different symmetry permits accounting for the anisotropy of the elastic constant matrix. However, the period of the grant expired before the spectra on the modified spectrometer could be obtained.

Although the stiffness matrix could not be calculated directly from experimental data, an approximate set of elastic constants can be calculated using theoretical scattering data. The direction cosines of the phonon can be accurately calculated for any scattering geometry. Since the HMX optical indicatrix was measured, the refractive index along any incident or scattering direction can be calculated. This leaves the Brillouin shifts that can be well approximated by comparison to the large number of actual spectra taken from phonon scattering in the bc^* plane. From these Brillouin shifts, we have been able to calculate the approximate stiffness matrix (Fig. 3) which can also be used to calculate such properties as the bulk compressibility and Young's modulus.

$$C = \begin{bmatrix} 1.491 & -.353 & .205 & 0 & .040 & 0 \\ -.353 & 1.790 & -1.044 & 0 & -.031 & 0 \\ .205 & -1.044 & 1.651 & 0 & -.135 & 0 \\ 0 & 0 & 0 & .785 & 0 & .209 \\ .040 & -.031 & -.135 & 0 & .621 & 0 \\ 0 & 0 & 0 & .209 & 0 & 1.06 \end{bmatrix} \times 10^{10} \frac{N}{m^2}$$

Figure 3: Approximate Stiffness Matrix for β -HMX

Theory of Initiation of Detonation

Over the period of the grant, collaboration with Prof. Tadeusz Luty of the Technical University of Wrocław was actively focused on formulation of a quantitative microscopic model for detonation. Given the breadth of the subject, the focus was specifically on how mechanical energy is directly converted into chemical energy at the very initial stage of detonation where the shock wave traverses the unreacted and previously unperturbed molecules in the crystal. A microscopic model dealing with this phase of detonation may be expected to be useful to synthetic and materials chemists in the design, synthesis and production of new energetic materials.

The model that was developed is based on the idea of Gilman¹⁰ that a molecule does not have time to mechanically respond to the shock wave through its vibrational degrees of freedom but rather must take up the available energy by closing the highest occupied molecular orbital-lowest occupied molecular orbital (HOMO-LUMO) gap. However, it is less restrictive and does not require complete closure of the gap and subsequent metallization to explain how the mechanical energy is converted to molecular excitation and reaction. The theory shows that the deformation potential of the molecule, Φ_{def} , is the crucial physical property and that this determines the degree to which the HOMO-LUMO gap must decrease to lead to an initial chemical response to the shock wave.

Our theory for mechanochemical induced processes was published in the *J. Chem. Phys.*¹¹ The treatment shows that the initial response of a molecule to a shock wave requires the molecule to distort to a geometry that is essentially the “ground state” of the molecule suffering the extremely high effective pressure of the shock wave. A new insight in this treatment is the representation of the distortion of the molecule by a linear combination of normal mode coordinates. This “compressed ground state” arises from mixing of the ambient ground-state potential of the molecule in the crystal with a dissociative excited state potential. The combination of these two diabats to form the “high-pressure ground state” is represented in Figure 4.

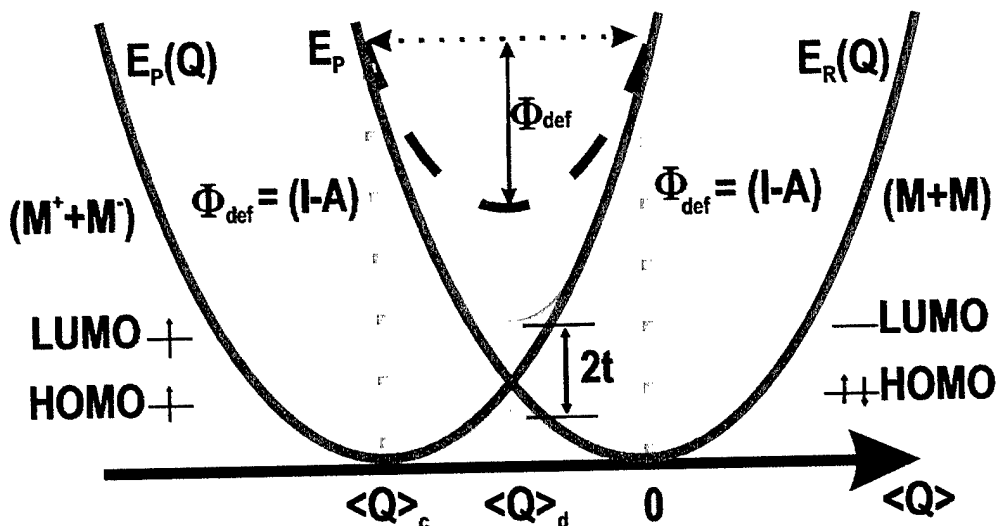


Figure 4: Diabats for mixing of states for a molecule under significant stress. Q_c is the normal coordinate representing some critical deformation while Q_d is the value of that coordinate for the deformation mixing. LUMO and HOMO are the Lowest Unoccupied Molecular Orbital and Highest Occupied Molecular Orbital, respectively. I is the ionization potential and A is the electron affinity. M represents the molecule in various valence states. Φ_{def} is the deformation potential and t is the energy of the gap between the new states arising from mixing. E_p and E_r are the energies of the product and reactant molecular species.

The height of the barrier, Φ_{def} , is related to how easily the molecule can be deformed and thus, is obviously specific to a given molecule. If there is excess mechanical energy, then the molecule can be forced over the barrier to produce products that will be essentially those associated with the mixing dissociative state but there will be products that also relate to thermal decompositon of the bound ground state. Thus, the mechanical energy is used to deform a molecule to yield the illustrated potential. If there is excess mechanical energy beyond that required for this deformation, the molecule can traverse the potential barrier to produce products consistent with those of the two diabats. The model thus explains why photochemical products of the energetic materials are observed as detonation products.

Another way to understand the process is by analogy to the reaction rate theory of Marcus. In the illustration [Fig. 5] the mixing of the “reacting” states, in this case the ground state and the excited state that is accessed because of compression driving the molecule up the repulsive part of its ground state potential, is shown on the left in common representation but on the left the plot is that of the resulting high stress “ground state” represented in a reaction coordinate plot.

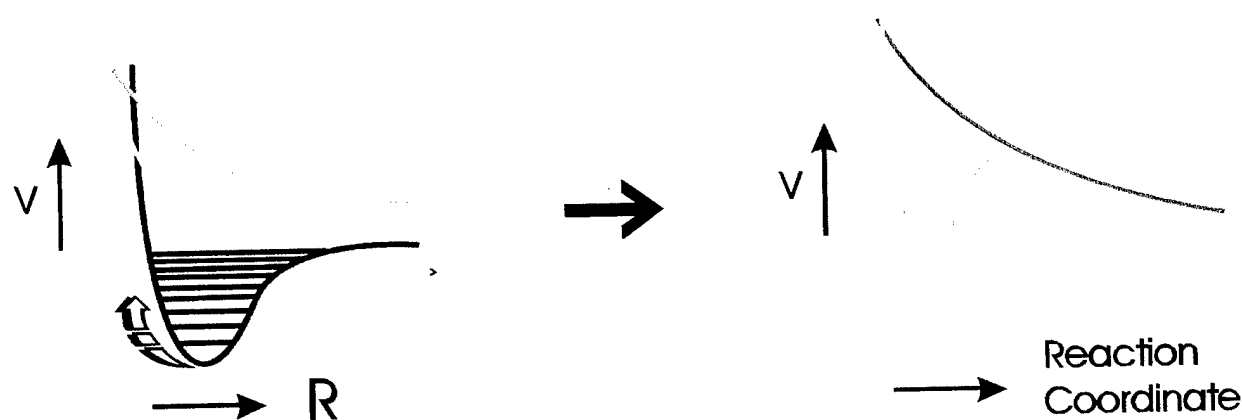


Figure 5 Representation of compressive excitation of ground state to intersection with higher energy state where mixing may occur (left) and showing reactive nature of the resulting high pressure “ground state” as a reaction coordinate diagram (right).

Hot Spots

The role of “hot spots,” regions of the crystal of the energetic material that appear to be involved “prematurely” in the initial detonation process, has been of interest for some time. The idea that such “hot spots” are associated with lattice defects has long standing. This model gives quantitative expression to this qualitative idea.

Because defects are invariably associated with a strain field, molecules in the region of the defect are already under some tension, perhaps enough to distort them to the stress-induced state of Fig. 5 (right). Such molecules are already “on their way” to passing over the barrier and subsequent formation of detonation products. The height of this barrier is the deformation potential and, since the strain field is already contributing to the distortion of the molecules in its region, such molecules are already possessed of the energy needed for reaction. Alternatively, even if the molecule is not

initially in the “compressed ground state” it is already in a sufficiently strained region that it does not require as much energy as a molecule in a strain-free region requires to satisfy the need of sufficient energy to surmount the Φ_{def} barrier. Such molecules will thus be the first to decompose. Either way, the model accounts for “hot spots” and substantiates the view they are associated with defects.

“Inverse” Jahn-Teller Effect

A further result of the mechanochemical theory is that symmetry arguments based on the equations show that high-symmetry molecules are necessarily more unstable to mechanical stress. This may be thought of as the molecule reacting to the imposed stress but unable to accommodate the stress by deformation and thus only being able to achieve relief by bond scission. This has been seen in a full ab initio calculation¹² that shows RDX breaks only one N-N breaks in the initial process. We were able to confirm this by a DFT calculation based on our model. However, the operant principle is that of symmetry and it has a direct message for chemists regarding the role of symmetry in the design of energetic materials for explosives.

Although the subsequent fate of the energy, formation of the detonation wave, etc. was not addressed in this theoretical work, the aspects that may be argued to be most useful to the synthetic chemist trying to design a new explosive are delineated. This can only be achieved from a microscopic understanding of all of the processes involved in detonation. This particular model produces a “zeroth-order” microscopic picture that can be used in rational design of energetic materials.

REFERENCES

1. M. Rey-Lefon, et al., *J. Chim. Phys. Phys.-Chim. Biol.* (1971) **68**, 1533; *ibid.*, 1573.
2. C.S. Choi, et al., *Acta Cryst.* (1970) **B26**, 1235.
3. Z. Iqbal, et al., *J. Chem. Phys.* (1974) **60**(1), 221.
4. M. R. Cavagnat, et al., *C. R. Acad. Sc. Paris* (1971) **273**, 658.
5. T. B. Brill, et al., *J. Phys. Chem.* (1979) **85**(3), 340.
6. Sorescu, et al., *J. Phys. Chem. B* (1997) **101**, 798.
7. G. D. Smith, et al., *J. Phys. Chem. B* (1999) **103**, 3570.
8. A. Gavezzotti, et al., *Acc. Chem. Res.* (1994) **27**(10), 308.
9. J. M. Rosen, et al., *J. Chem. Eng. Data* (1969) **14**, 120.
10. J. J. Gilman, *Phil. Mag.* (1999) **B79**, 643 and references therein.
11. T. Luty, P. Ordon, C. J. Eckhardt, *J. Chem. Phys.* (2002) **117**, 1775.
12. C. J. Wu, L. E. Fried, *J. Phys. Chem.* (1997) **101**, 8675.